4th URSI AT-RASC, Gran Canaria, 19 – 24 May 2024

Highly Directive Holey Photonic Crystal Leaky-Wave Antennas using Low-Permittivity Materials

Ludovica Tognolatti(1), Vakhtang Jandieri(2), Cristina Ponti(1),
Giuseppe Schettini(1), and Paolo Baccarelli(1)
(1) Department of Industrial, Electronic, and Mechanical Engineering, Roma Tre University, 00146 Roma, Italy
(2) Department of General and Theoretical Electrical Engineering (ATE), Faculty of Engineering, University of Duisburg-Essen, and CENIDE – Center for Nanointegration Duisburg-Essen, D-47048 Duisburg, Germany

Abstract

This contribution systematically explores the radiation from an electric line source within dielectric photonic crystals. These structures consist of periodic chains of circular voids in dielectric media. It is demonstrated how this category of holey lattices has the potential to be employed in designing leaky-wave antennas that exhibit high directivity. The possibility of decreasing the relative permittivity of the hosting dielectric medium by preserving leaky-wave radiative properties, such as beam focusing and radiation efficiency, is investigated. This offers notable benefits in terms of additive manufacturing, simple design, and low overall complexity. Finally, two examples of realistic three-dimensional holey photonic crystal leaky-wave antennas are presented in this paper.

1 Introduction

The focused emission from dielectric photonic crystals (PCs) [1] was initially studied by using geometric-optics considerations [2]-[4], in the case of embedded sources operating at the lowest edge of the air band. A leaky-wave formalism was employed to explain the radiative phenomenology, mainly when homogenized structures were considered [5, 6], but also in PCs and quasicrystals [7, 8]. The radiation mechanism of two-dimensional (2-D) dielectric lattices has been extensively investigated in terms of leaky modes [9], presenting a procedure based both on the analysis of the band diagrams of the Bloch waves propagating in the 2-D PCs and the leaky-wave investigation of open periodic waveguides. This provided an interesting perspective on antenna design. The leaky-wave radiation from dielectric rod PCs (DRPCs) as well as holey PCs (HPCs), made by 2-D periodic lattices of circular dielectric rods in free space and air columns drilled in a dielectric hosting medium, respectively, was considered in [10]. HPCs were identified as the best candidate to achieve high directive radiation, with performance 6 dB higher than those based on DRPCs. In this contribution, further important details and guidelines for the design of highly directive HPC leaky-wave antennas (HPCLWAs) bisected by a metal plate are provided. In particular, it is shown how high directivity is maintained even when the relative permittivity of the hosting dielectric medium is decreased and the total band gap of the 2-D PC vanished. This is of considerable interest from a manufacturing point of view, because it allows the use of low-cost techniques such as three-dimensional (3-D) printing [11]. Finally, two novel examples of 3-D HPCLWAs, designed to operate at $f = 24$ GHz, are presented.

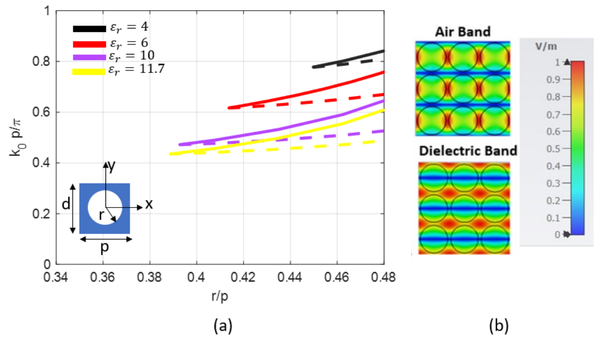

Figure 1. (a) Gap maps for TE Bloch modes in terms of normalized frequencies at the lower edge of the air band (thick lines) and at the higher edge of the dielectric band (dashed lines) as a function of r/p for different values of dielectric permittivities for a square lattice of air columns. Here r is a radius of the cylinder, p is a period of the structure, and k_0 is the free-space wavenumber. (b) The magnitude of the z- component of the electric Bloch modal fields E_z at the air band and at the dielectric band.

2 Gap maps for a square lattice of circular air columns and open waveguides composed by periodic chains of voids

The band diagrams of Bloch waves propagating in the 2-D PC, depicted in Fig. 1 (a), represent a significant tool for understanding the physical characteristics and conducting an initial design of antennas based on 2-D dielectric lattices. In [2] it was shown that the lowest edge of the second band, also referred to as the air band, is a good working point to get the lattice to behave as a spatial filter and focus the radiation. Gap maps in terms of normalized frequency versus r/p ratio, where r is the radius of the cylinder and p is the period of the structure (here and in the following

$d = p$), are obtained by using the CST Eigenmode Solver and are shown for typical dielectric permittivities in Fig. 1 (a). It can be observed that in the air bands the magnitude of the electric field presents a null exactly in the middle of the dielectric region between two voids (see Fig. 1 (b)).

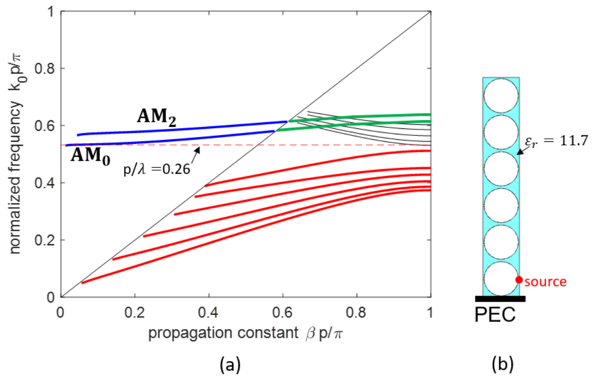

Figure 2. (a) Brillouin diagram for the TE modes of an open waveguide with $N_y = 6$ periodic chains of air columns, with $r/p = 0.45$ and $\varepsilon_r = 11.7$. The forward (bound) dielectric modes at lower frequencies are indicate with red lines, while the corresponding backward modes at higher frequencies as black dotted lines. The first two forward air modes are indicated with green (bound modes) and blue (improper leaky modes) lines. The horizontal dashed line indicates the operating normalized frequency. (b) The unit cell of the structure and the position of the line source.

Moreover, it is possible to note that, as the dielectric constant decreases, the band-gap decreases until it totally disappears for dielectric constants less than $\varepsilon_r = 4$. However, an effective alternative approach was considered in [9], where photonic crystal dielectric structures were considered as open waveguides composed of a stack (along the transverse direction) of infinite periodic chains. The advantage of this approach is that the used model better matches the physics of the ideal radiator and the radiative behaviors of the antenna can be rigorously described in terms of leaky modes. An open waveguide composed by a stack of N_y infinite periodic chains of air columns drilled in a dielectric slab has been considered as a basic model of HP-CLWA [10]. The Brillouin diagram of a structure composed by $N_y = 6$ periodic chains, $r/p = 0.45$, and dielectric constant $\varepsilon_r = 11.7$, is shown in Fig. 2. Six forward dielectric modes, one for each periodic chain, are observed at low frequencies (red lines), the sixth being a plasmonic mode with modal field highly confined between the free space and the dielectric medium. At higher frequencies forward air modes (green lines) and backward dielectric modes (black lines) are present. The two improper leaky modes AM_0 and AM_2, obtained by using the rigorous full-wave modal solver developed in [12], are shown in blue. Maximum directivity is achieved through the leaky AM_0 mode excited at the normalized frequency indicated as a dashed line in Fig. 2. In order to maximize radiation efficiency and avoid edge diffraction effects in realistic truncated (non infinite) structures, bound modes of the open waveguide should not be excited. Here, even if backward guided modes are present at this operating frequency, they cannot be excited by properly placing the line source excitation, since the modal configurations of the backward modes at the higher edge of the closed stopband have a deep minimum exactly where the leaky air modes present a strong maximum (see Section III.C in [10] for further details). Finally, also the plasmonic mode could be not excited by a source placed sufficiently far from the top of the open waveguide structure.

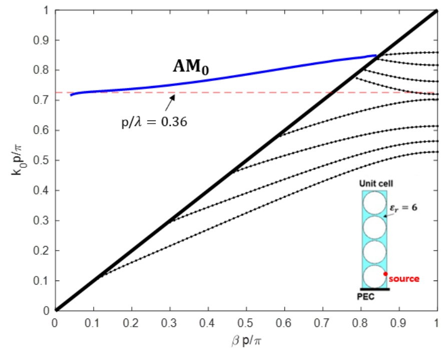

Figure 3. Brillouin diagram for the TE modes of an open waveguide with $N_y = 4$ periodic chains of air columns with $r/p = 0.46$ and $\varepsilon_r = 6$. The horizontal dashed line indicates the operating normalized frequency. The blue solid line indicates the leaky AM_0. In the inset the unit cell of the structure and the position of the line source are reported.

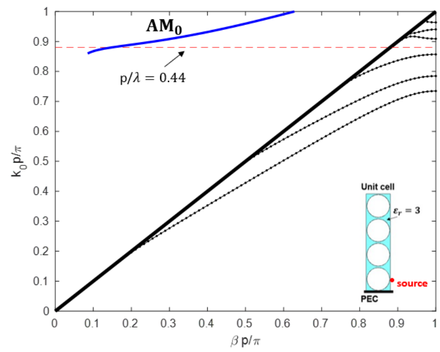

Figure 4. Brillouin diagram for the TE modes of an open waveguide with $N_y = 4$ periodic chains of air columns with $r/p = 0.45$ and $\varepsilon_r = 3$. The horizontal dashed line indicates the operating normalized frequency. The blue solid line indicates the leaky AM_0. In the inset the unit cell of the structure and the position of the line source are reported.

3 3-D HPCLWAs design and discussion

Here, we consider an holey photonic crystal structure consisting of $N_y = 4$ periodic chains of air columns drilled in a grounded dielectric slab with dielectric permittivity $\varepsilon_r = 6$ (see the insert of Fig. 3). The ratio between the radius of the holes and the period of the structure is $r/p = 0.46$. Fig. 3 shows the Brillouin diagram for the TE guided modes and the radiative leaky AM_0 of the structure obtained with CST Eigenmode Solver. The normalized com-

Table 1. Maximum directivity values and the normalized frequencies at which are obtained for several cases.

	$\varepsilon_r = 3$	$\varepsilon_r = 6$
$\mathbf{N_y = 4}$	$p/\lambda = 0.44$	$p/\lambda = 0.36$
	$r/p = 0.45$	$r/p = 0.46$
	$D = 11.6$ dB	$D = 12.7$ dB
$\mathbf{N_y = 8}$	$p/\lambda = 0.42$	$p/\lambda = 0.37$
	$r/p = 0.45$	$r/p = 0.46$
	$D = 14.6$ dB	$D = 17.4$ dB

plex leaky AM_0 wavenumber at $p/\lambda = 0.363$ (see the horizontal dashed line in Fig. 3), which corresponds to maximum simulated directivity when the source is placed as in the inset of Fig. 3, is $k_x/k_0 = 0.099 - j0.147$. It is possible to observe how, considering lower dielectric constants, the modes have shifted to higher frequencies, but we still maintain, for this case, a significant band-gap. A second structure consisting of $N_y = 4$ periodic chains of air columns drilled in a grounded dielectric slab, with $\varepsilon_r = 3$ and $r/p = 0.45$, is considered. The unit cell is shown in the inset of Fig. 4, where the Brillouin diagram is illustrated. In this case, as we commented in Section II, we do not have a total band gap in the 2-D band diagram since the permittivity is too low. However, the Brillouin diagram of the transversely open waveguide in Fig. 4 clearly shows that at the operating frequency $p/\lambda = 0.44$ (see the horizontal dashed line in Fig. 4), where maximum directivity is achieved, we do not observe bound propagating modes, since the higher order plasmonic forward mode is below cutoff and the backward ones are still in stopband (moreover they would be not excited by a proper choice of the source location). Furthermore, a leaky AM_0 is still present and the normalized complex leaky-mode wavenumber at $p/\lambda = 0.44$ is $k_x/k_0 = 0.1563 - j0.1612$. The maximum directivity values and the normalized frequencies at which they are obtained, for $\varepsilon_r = 3$ and $\varepsilon_r = 6$ are summarized in Tab. 1, also considering a higher number of periodic chains ($N_y = 8$). We observe that for both values of the relative permittivy the considered configurations show very high directive radiation.

Finally, two realistic holey 3-D HPCLWAs are designed. Illustrations and details of the 3-D truncated structures are shown in Fig. 5. At first we consider the case where $\varepsilon_r = 6$. We truncate the structure longitudinally on the basis on the knowledge of the attenuation constant of the dominant leaky mode AM_0, achieving a desired radiation efficiency $\eta_r = 90\%$ and sandwiching the HPC slab between two metal plates distant from each other by $\lambda/2$. The antenna is sized to operate at $f = 24$ GHz with dimensions 72.6×18.14 mm ($N_x = 4$, $N_y = 16$), as shown in Fig. 5. The chosen feeder is a standard coaxial cable. The comparison between the theoretical leaky-wave pattern, obtained through a standard analytical formulation for a truncated bidirectional LWA [13], and the CST total field at $f = 24$ GHz is shown in Fig. 6 (a). Very good agreement is obtained for the main radiating lobe and negligible diffraction by the edges is observable, as expecetd since bound modes are not excited and the leaky AM_0 reaches the antenna edges with less than 10% of the injected power. The reflection coefficient in the frequency band between $f = 23.5$ GHz and $f = 24.5$ GHz is shown in Fig. 6 (b). At $f = 24$ GHz it assumes a value of $|S_{11}| = -15.6$ dB.

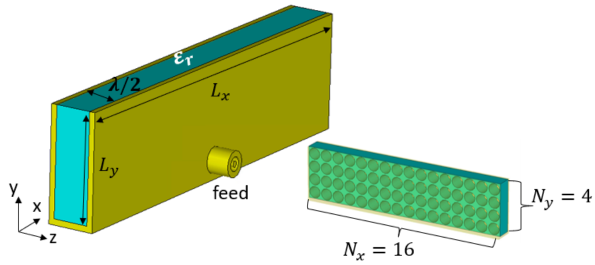

Figure 5. Illustrations and details of the 3-D truncated structure. The design frequency is 24 GHz. The dielectric constant of the first structure considered is $\varepsilon_r = 6$. The dimensions are: $L_x = 72.6$ mm, $L_y = 18.14$ mm. The dielectric constant of the second structure is $\varepsilon_r = 3$. The dimensions are: $L_x = 87.94$ mm, $L_y = 21.99$ mm.

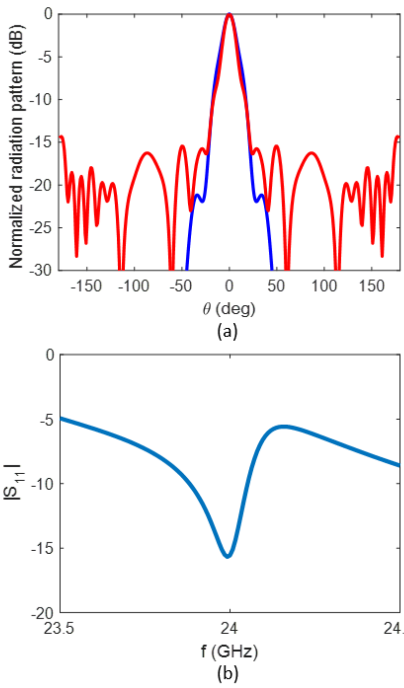

Figure 6. (a) Comparison between the leaky AM_0 and the CST total field of the first structure ($\varepsilon_r = 6$, $L_x = 72.6$ mm, $L_y = 18.14$ mm) at $f = 24$ GHz ($p/\lambda = 0.363$). (b) Amplitude in dB of the reflection coefficient.

As a second case we consider the structure with $\varepsilon_r = 3$. Based on the knowledge of the attenuation constant, we truncate longitudinally the antenna ($N_y = 16$) to have a radiation efficiency of $\eta = 92\%$. The dimensions of the antenna, sized to operate at $f = 24$ GHz, are 87.94×21.99 mm. Fig. 7 (a) shows very good agreement between the

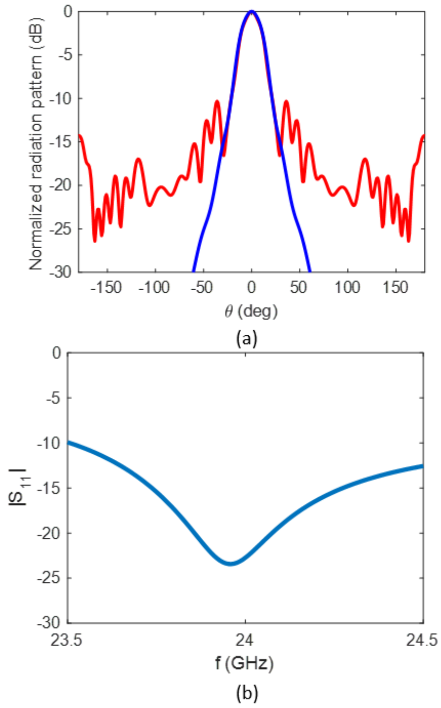

Figure 7. (a) Comparison between the leaky AM_0 and the CST total field of the structure ($\varepsilon_r = 3$, $L_x = 87.94$ mm, $L_y = 21.99$ mm) at $f = 24$ GHz ($p/\lambda = 0.44$). (b) Amplitude in dB of the reflection coefficient.

leaky AM_0 and the CST total field at $f = 24$ GHz and an almost complete absence of radiation from antenna edges. The reflection coefficient in the frequency band between $f = 23.5$ GHz and $f = 24.5$ GHz is shown in Fig. 7 (b). At $f = 24$ GHz it assumes a value of $|S_{11}| = -22.7$ dB. It is thus shown that even in the absence of a complete stopband in the 2-D PC band diagram, it is still possible to properly design a directive HPCLWA, by carefully investigating the leaky and bound modes of the relevant open waveguide. For this low-permittivity configuration, in addition to the advantage of using dielectrics that can be easily modeled with commercial 3-D printers [11], we also achieve a larger matching bandwidth, as can be observed in Fig. 7 (b).

4 Acknowledgements

This work was supported by the Ialian Research Project of National Relevance PRIN 2017 WPT4WID.

References

[1] J. D. Joannopoulos, S. G. Johnson, J. N. Winn, and R. D. Meade, *Photonic Crystals: Molding the Flow of Light, 2nd ed., Princeton*, NJ, USA: Princeton Univ. Press, 2008,

[2] S. Enoch, G. Tayeb, and D. Maystre, "Dispersion diagrams of Bloch modes applied to the design of directive sources," *Prog. Electromagn. Res.*, vol. 41, pp. 61–81, 2003.

[3] S. Enoch, G. Tayeb, P. Sabouroux, N. Guérin, and P. Vincent, "A metamaterial for directive emission," *Phys. Rev. Lett.*, vol. 89, no. 21, 2002, Art. no. 213902.

[4] S. Enoch, G. Tayeb, and B. Gralak, "The richness of the dispersion relation of electromagnetic bandgap materials," *IEEE Trans. Antennas Propag.*, vol. 51, no. 10, pp. 2659–2666, Oct. 2003.

[5] G. Lovat, P. Burghignoli, F. Capolino, D. R. Jackson, and D. R. Wilton, "Analysis of directive radiation from a line source in a metamaterial slab with low permittivity," *IEEE Trans. Antennas Propag.*, vol. 54, no. 3, pp. 1017–1030, Mar. 2006.

[6] P. Burghignoli, G. Lovat, F. Capolino, D. R. Jackson, and D. R. Wilton, "Directive leaky-wave radiation from a dipole source in a wire-medium slab," *IEEE Trans. Antennas Propag.*, vol. 56, no. 5, pp. 1329–1339, May 2008.

[7] A. Della Villa, V. Galdi, F. Capolino, V. Pierro, S. Enoch, and G. Tayeb, "A comparative study of representative categories of EBG dielectric quasicrystals," *IEEE Antennas Wireless Propag. Lett.*, vol. 5, pp. 331–334, 2006.

[8] A. Micco et al., "Directive emission from defect-free dodecagonal photonic quasicrystals: A leaky wave characterization," *Phys. Rev. B*, vol. 79, no. 7, 2009, Art. no. 075110.

[9] P. Baccarelli, L. Tognolatti, V. Jandieri, S. Ceccuzzi, C. Ponti, and G. Schettini, "Leaky-wave radiation from 2-D dielectric lattices excited by an embedded electric line source," *IEEE Trans. Antennas Propag.*, vol. 69, no. 11, pp. 7404–7418, Nov. 2021.

[10] L. Tognolatti, V. Jandieri, S. Ceccuzzi, C. Ponti, G. Schettini and P. Baccarelli, "Highly Directive Leaky-Wave Radiation in 2-D Dielectric Photonic Crystals," in *IEEE Antennas Wirel. Propag. Lett.*, vol. 22, no. 4, pp. 819-823, Apr. 2023.

[11] A. Goulas, et. al., "Synthesis and dielectric characterisation of a low loss BaSrTiO3/ABS ceramic/polymer composite for fused filament fabrication additive manufacturing", *Additive Manufacturing*, vol. 55, pp. 102844, 2022.

[12] V. Jandieri, P. Baccarelli, G. Valerio, and G. Schettini, "1-D periodic lattice sums for complex and leaky waves in 2-D structures using higher order Ewald formulation", in *IEEE Trans. Antennas Propag.*, vol. 67, n. 4, pp. 2364-2378, 2019.

[13] D. R. Jackson and A. A. Oliner, *Leaky-Wave Antennas Modern Antenna Handbook.* C. A. Balanis, Ed., Hoboken, NJ, USA: Wiley, 2008, ch. 7, pp. 325–367.